ARID ZONE JOURNAL OF ENGINEERING, TECHNOLOGY & ENVIRONMENT
AZOJETE June 2021. Vol. 17(1):121-140
Published by the Faculty of Engineering, University of Maiduguri, Maiduguri, Nigeria.
**Print ISSN: 1596-2490, Electronic ISSN: 2545-5818**
www.azojete.com.ng

**ORIGINAL RESEARCH ARTICLE**

# NEW REFINED SHEAR DEFORMATION THEORY EFFECT ON NON-LINEAR ANALYSIS OF A THICK PLATE USING ENERGY METHOD

**F. C. Onyeka[1] and T. E. Okeke[2]***
[1]Department of Civil Engineering, Edo University, Iyamho. Edo State, Nigeria.
[2]Department of Civil Engineering, University of Nigeria, Nsukka, Enugu State, Nigeria

*Corresponding author's email address: onyeka.festu@edouniversity.edu.ng

**ARTICLE INFORMATION**

Submitted 25 Oct., 2020
Revised 2 January 2021
Accepted 8 January 2021

**Keywords:**
Direct energy method
trigonometric displacement function
polynomial shear deformation
new refined plate theories
SSFS rectangular plate

**ABSTRACT**

*This study presents the application of a new refined plate theory in the bending analysis of a thick rectangular plate carrying a uniformly distributed load using the direct energy method. The new refined plate theory which is a combination of trigonometric shear deformation theory and fourth order polynomial displacement function was used to formulate the governing differential equation by employing the principle of elasticity. The total potential energy equation of a thick plate was formulated from the constitutive relations thereafter the three general governing differential equations for the determination of the deflection and shear deformations rotation along the direction of x and y coordinates were obtained. The coefficient of deflection and shear deformation were derived by subjecting the energy equation obtained to direct variation thereafter the actual deflection, in-plane displacement, normal and shear stresses, moment and stress resultants of the rectangular thick plate were determined by substituting the derived coefficient of coefficient of deflection and shear deformation into the displacement, shear force, moment and stresses deduced. The particular plate boundary condition to be anlysed is free support at the third edge and the other three edges simply supported (SSFS). The result shows that thick plate is the one whose span-depth ratio value is 4 up to 25. The results obtained from this work was compared with those obtained from other refined plate theories with the same support condition and obtained showed good agreement with those in the literature*



## 1.0 Introduction

A plate isdescribed as structural components with thickness smaller than its surface dimensions (Shwetha and Subrahmanya (2018). Plates have been widely applied in aerospace engineering, structural and mechanical engineering, etc., in building and constructing many engineering structures and elements like aircraft wings, ships, buildings, bridges, roof, retaining walls, railways, turbine disks etc. (Onyechere *et al.,* 2020; Ozioko *et al.,* 2019; Onyeka *et al.,* 2018). Plates have been classified based on thickness (t) as; thin and thick plates (Chandrashekhara 2001). The edges of plate can have different support conditions which can be fixed, simply supported, point, etc. There has been a great deal of research on bending analysis of plates from various scholars using theorems with different boundary support conditions. It is the depth of plate that mainly affects the bending properties of plate compared with its other dimensions like the length and width (Gujar and Ladhane, 2015; Ibearugbulem *et al.,* 2013).

The analysis of plates involves finding the normal and shear stresses, displacement, moments etc., at different points of the plate and it is necessary as it helps to ascertain the plate stability and ability to withstand design loads (Roknuzzaman, 2015). The loads which are either static or dynamic carried by plates are mostly perpendicular to the faces of the plate, and the load carrying capacity of the plate is similar to that of beams as a structural element. Plate theory generally known as the classical plate theory (CPT) is commonly used in the analysis of thin plates. The CPT was formulated by Kirchhoff (1985) and was applied by Timoshenko and

Woinowsky (1959) and Liessa (1973) for the analysis of plates and shells.

The CPT theory, which does not address shear deformation transversely as seen in the thin plate, is based on the assumption that the normal to the mid-surface remains normal before and after deformation. Due to the non-inclusion of transverse shear strains or deformation in CPT, it has been found to be inadequate in the analysis of thick plates (Ibearugbulem *et al.*, 2016). To address the short fall in the CPT, researchers formulated the Refined Plate Theory (RPT). This includes, the First Order Shear Deformation Theory (FSDT) (Reissner, 1945; Hoang *et al.*, 2019), Second Order Shear Deformation theory (SSDT) and the Higher Order Shear Deformation Theories (HSDT) which considers transverse shear deformation (Sayyad *et al.*, 2017), in the analysis of plates, using different functions like: trigonometric, exponential, polynomial.

Aghdam and Vafa (2004) researched on bending solutions of rectangular thick plates by the application of the extended Kantorovich method (EKM). The EKM involves eight unknowns which were solved using governing equations based on Reissner FSDT. They concluded that the application of EKM in the thick plate's analysis was fast and gave similar results for plates analyzed by finite element method (FEM).

Sayyad (2013) worked on the flexural analysis of orthotropic thick plates using refined plate theory which takes into account transverse shear deformation effect. They obtained the in plane displacement field using an exponential function which was based on broadness coordinate, the transverse shear stress directly from the constitutive without the need for shear correction factor, while the governing equations and boundary conditions were based on the virtual work principle. The results of the displacements, stresses, and frequencies obtained, when compared with results from other plate theory and exact theory were found to be adequate.

Ghugal and Gajibhiye (2016) did a study on the analysis of thick isotropic plates in rectangular relation to bending with simply supported supports using a form of higher order shear deformation theory (HSDT). They obtained the transverse normal strain deformation effect, and the proposed displacement field which accounted for non-linear variation of in-plane displacements, stresses and the transverse displacements with the plate thickness without the need for correction factor which is seen in FSDT. The numerical results which include static flexure analysis were done with MATLAB programming and with the results agreed with other HSDT and exact 3D elasticity solutions.

Sayyad *et al.* (2015) worked on thermos-elastic bending examination of laminated plates with matrix reinforced materials, simply supported on all four edges and acted upon by a heat related loads changing linearly with the plate's depth according to various shear deformation theories. They investigated thermal related deformations using a combined approach that involved different functions in relation to thickness coordinate and shear deformation effects. The displacements and stresses they predicted by PSDT, TSDT, and HSDT were similar with each other, but FSDT gave higher results of in-plane normal stress compared to other.

Zhong and Qian (2017) worked on the bending analysis of thick plate with geometry and with all ends clamped (CCCC) at supports. They used governing equations derived from the Mindlin's plate theory for their analysis. They found out that their proposed method of analysis eliminates the complex derivation for obtaining coefficients and gave accurate results.

Ibearugbulem *et al.* (2018) did a study on the analysis of rectangular thick plate in relation to bending with all the plate's supports clamped (CCCC) by applying polynomial shear deformation theory (PSDT). They used a theory formed from Ritz energy method with a displacement function relating to a polynomial function in their analysis. They obtained the transverse shear stress without the need for shear correction factor, with the total potential energy equation formulated from the principle of electricity. They concluded their study by comparing their results for: displacements and stresses with other studies, and found out that there were similarities.

Eze *et al.* (2018) investigated the use of shear deformation theory in analyzing rectangular isotropic thick plate with two different boundary conditions. They derived a theory for determining shear deformation without the need for correction factor, and displacement coefficients by using total potential energy in direct variation on the boundary conditions of: simply support at the third edge with other three edges clamped (CCCS) and fixed at the third edge with other three edges simply supported (SSFS) respectively. The results they obtained were satisfactory results when compared with results from other studies.

Onyeka and Edozie (2020) analyzed the moments and stresses of thick rectangular plate with clamped at three edges and simply supported at the remaining one edge (CCCS) and subjected to uniformly distributed load, using third order shear deformation theory by formulating the total potential energy equation. Their formulated theory which didn't put shear correction factor into consideration gave mathematical expressions for the determining maximum deflection, moment, stresses and in-plane displacements. Their theory was error free when they carried out numerical comparism with other studies.

Literatures reveals that there have been a lot of research efforts by many researchers on the bending analysis of plates using different shear deformation theories based on different mathematical functions and not energy method in determining the bending effects of thick plate that are rectangular in nature with support conditions of different kinds. This study is aimed at addressing this gap in literatures by presenting a new refined plate theories (NRPT) using energy method to obtain the deflection, moment, stress, in – plane displacements of thick plate with rectangular geometry under uniformly distributed loads with free support at the third edge and the other three edges simply supported (SSFS). This NRPT circumvent the use of shear correction factor which is associated with first order shear deformation theory.

## 2. Materials and Methods

Following the sketch as presented in Figure 1 and the assumption made as shown below, the governing equation of thick plate under pure bending is made.

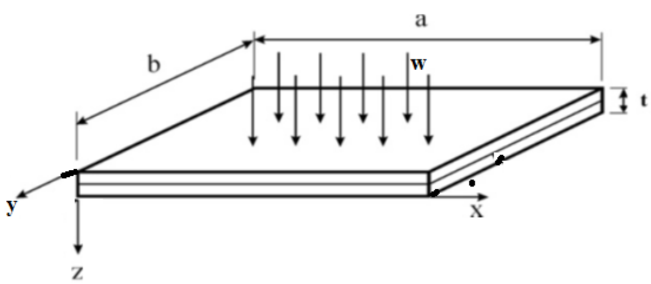


**Figure 1:** A rectangular thick plate element carrying a uniformly distributed load

## 2.1. Assumptions

Considering the following assumptions, the general governing equation of a thick rectangular plate will be formulated. They include:

I. The material of the plate is homogeneous, isotropic and elastic.
II. The strain and stress normal to x-y plane is so small that it can be neglected.
III. The vertical line that is initially normal to the middle surface of the plate before bending is no longer straight nor normal to the middle surface after bending.

## 2.2. Kinematics and Constitutive Relationships

In the formulation of the kinematics and constitutive relation, the in-plane displacement components along x-axis $(u)$ and in-plane displacement components along y axis $(v)$ are derived by Onyeka *et al.* (2020) as presented in the equations (1) and (2) :

$$u = \frac{zd\cup}{dx} + S(z).\cap_x \tag{1}$$

$$v = \frac{zd\cup}{dy} + S(z).\cap_y \tag{2}$$

Let the shear deformation profile of plate section ($S(z)$) (Touratier, 1991) be:

$$S(z) = \frac{t}{\pi}\sin\left(\pi\frac{z}{t}\right) \tag{3}$$

and;

$\cap_x$ and $\cap_y$= shear deformation rotation along x and y axis

Considering the assumptions in the previous section (assumption II), the stress normal to the x-axes gives:

$$\varepsilon_x = \frac{du}{dx} \tag{4}$$

Similarly, the stress normal to the y-axes becomes:

$$\varepsilon_y = \frac{du}{dy} \tag{5}$$

The curvature in x-z plane is defined as:

$$\gamma_{xy} = \frac{du}{dy} + \frac{dv}{dx} \tag{6}$$

The curvature in x-z plane is defined as:

$$\gamma_{xz} = \frac{du}{dz} + \frac{d\cup}{dx} \tag{7}$$

The curvature in x-z plane is defined as:

$$\gamma_{yz} = \frac{dv}{dz} + \frac{d\cup}{dx} \tag{8}$$

The constitutive Equations for five stress and strain components according to Onyeka *et al.* (2020) includes:

The normal stress along the direction of x-axes:

$$\sigma_x = \frac{E\left(\varepsilon_x + \mu\varepsilon_y\right)}{1-\mu^2} \tag{9}$$

The normal stress along the direction of y-axes:

$$\sigma_y = \frac{E\left(\varepsilon_y + \mu\varepsilon_x\right)}{1-\mu^2} \tag{10}$$

The shear stress along (x-y), (x-z) and (y-z) respectively are given in the Equation (1), (2) and (3) respectively as:

$$\tau_{xy} = \frac{E}{2(1+\mu)}.\gamma_{xy} \tag{11}$$

$$\tau_{xz} = \frac{E}{2(1+\mu)}.\gamma_{xz} \tag{12}$$

$$\tau_{yz} = \frac{E}{2(1+\mu)}.\gamma_{yz} \tag{13}$$

Where;

$\mathrm{E} = \text{Modulus of Elasticity and } \mu = \text{poison ratio}$

Substituting Equation (1), (2), (4) and (5) into Equation (9), we have:

$$\sigma_x = \frac{E}{1-\mu^2}\left[\left(-\frac{zd^2 \cup}{dx^2} + \frac{Sd \cap_x}{dx}\right) - \mu\left(\frac{zd^2 \cup}{dy^2} + \frac{Sd \cap_y}{dy}\right)\right] \tag{14}$$

Substituting Equation (1), (2), (4) and (5) into Equation (10), we have:

$$\sigma_y = \frac{E}{1-\mu^2}\left[\left(-\frac{zd^2 \cup}{dy^2} + \frac{Sd \cap_x}{dx}\right) - \mu\left(\frac{zd^2 \cup}{dx^2} + \frac{Sd \cap_y}{dy}\right)\right] \tag{15}$$

Substituting Equation (1), (2) and (6) into Equation (11), we have:

$$\tau_{xy} = \frac{E(1-\mu)}{(1-\mu^2)}\left[-\frac{z\partial^2 \cup}{\partial x \partial y} + S\left(\frac{d \cap_x}{dy} + \frac{d \cap_y}{dx}\right)\right] \tag{16}$$

Substituting Equation (1), (2) and (7) into Equation (12), we have:

$$\tau_{xz} = \frac{E(1-\mu)}{(1-\mu^2)}\left[\frac{z\partial^2 \cup}{\partial x \partial z} + S\left(\frac{d \cap_x}{dz} + \frac{d \cap_z}{dx}\right)\right] \tag{17}$$

Substituting Equation (1), (2) and (8) into Equation (13), we have:

$$\tau_{yz} = \frac{E(1-\mu)}{(1-\mu^2)}\left[\frac{z\partial^2 \cup}{\partial y \partial z} + S\left(\frac{d \cap_y}{dz} + \frac{d \cap_z}{dy}\right)\right] \tag{18}$$

## 2.3. General Energy Equation

The total potential energy expression (∄), was formulated in accordance with the kinematics and constitutive relation in the previous section (Onyeka *et al.*, 2018).

$$∄ = \Delta + \nabla \tag{19}$$

where:

$$\nabla = -\int_0^a \int_0^b w \cup (x,y) \partial x \partial y \tag{20}$$

where w is the uniformly distributed load.

$$\Delta = \frac{1}{2}\iiint_{-\frac{t}{2}}^{\frac{t}{2}} (\sigma_x\varepsilon_{x+}\sigma_y\varepsilon_{y+}\tau_{xy}\gamma_{xy} + \tau_{xz}\gamma_{xz} + \tau_{yz}\gamma_{yz})dxdydz \tag{21}$$

Thus:

$$\nexists = \frac{D}{2}\int_0^a\int_0^b \left[\left| g_1\left(\frac{\partial^2 \cup}{\partial x^2}\right)^2 - 2g_2\left(\frac{\partial^2 \cup}{\partial x^2}.\frac{\partial \cap_x}{\partial x}\right) + g_3\left(\frac{\partial \cap_x}{\partial x}\right)^2\right| + \left|2g_1\left(\frac{\partial^2 \cup}{\partial x\partial y}\right)^2 - 2g_2\left(\frac{\partial^2 \cup}{\partial x\partial y}.\frac{\partial \cap_x}{\partial y}\right) - 2g_2\left(\frac{\partial^2 w}{\partial x\partial y}.\frac{\partial \cap_y}{\partial x}\right)\right| + \left|(1+\mu)g_3\left(\frac{\partial \cap_x}{\partial y}\right)\left(\frac{\partial \cap_y}{\partial x}\right)\right| + \frac{(1-\mu)}{2}\left|g_3\left(\frac{\partial \cap_x}{\partial y}\right)^2 + g_3\left(\frac{\partial \cap_y}{\partial x}\right)^2\right| + \left|g_1\left(\frac{\partial^2 \cup}{\partial y^2}\right)^2 - 2g_2\left(\frac{\partial^2 \cup}{\partial y^2}.\frac{\partial \cap_y}{\partial y}\right) + g_3\left(\frac{\partial \cap_y}{\partial y}\right)^2\right| + \left|\frac{(1-\mu)}{2}g_4(\cap_x)^2 + \frac{(1-\mu)}{2}g_4(\cap_y)^2\right|\right]\partial x\partial y - \int_0^a\int_0^b w \cup (x,y)\partial x\partial y \tag{22}$$

## 2.4. Direct Governing Equation

The direct variational approach was applied to obtain the direct governing differential equation by differentiating the total potential energy with respect to the coefficient of deflection ($C$), coefficient of shear deformation with respect to x-axis ($C_x$) and coefficient of shear deformation with respect to y-axis ($C_y$).

In non-dimensional form, let:

$$z = ts;\ x = a \ni \text{ and } y = b \in \tag{23}$$

where:

a and b = length, breath and thickness of the plate

$\ni, \in$ and s = the non − dimensional value of length, breath and thickness of the plate

$$\text{Let the length to breath aspect ratio, } \alpha = \frac{b}{a} \tag{24}$$

$$\text{Span to thickness ratio, } \beta = \frac{a}{t} \tag{25}$$

Deflection ($\cup$), is the product of shape function of the plate and deflection coefficient:

$$\cup = C.n \tag{26}$$

where, $n$ is the shape function of the plate.

Similarly;

The shear deformation rotation along x-axis becomes:

$$\cap_x = \left[\frac{dn}{d\ni}\right][C_x] \tag{27}$$

Similarly, the shear deformation rotation along y-axis becomes:

$$\cap_y = \left[\frac{dn}{d\in}\right][C_y] \tag{28}$$

By substituting Equation 23, 24, 25, 26, 27 and 28 into 22, gives:

$$
\begin{aligned}
∄= \frac{Et^3}{24(1-\mu^2)a^4}\int_0^1\int_0^1 \Bigg[\Bigg|& g_1 C^2\left(\frac{\partial^2 n}{\partial \ni^2}\right)^2 - 2g_2 CC_x\left(\frac{\partial^2 n}{\partial \ni^2}\right)^2 + g_3 {C_x}^2\left(\frac{\partial^2 n}{\partial \ni^2}\right)^2\Bigg| \\
&+\left|2g_1\frac{C^2}{\propto^2}\left(\frac{\partial^2 n}{\partial \ni \partial \in}\right)^2 - 2g_2\frac{CC_x}{\propto^2}\left(\frac{\partial^2 n}{\partial \ni \partial \in}\right)^2 - 2g_2\frac{CC_y}{\propto^2}\left(\frac{\partial^2 n}{\partial \ni \partial \in}\right)^2\right| \\
&+\left|(1+\mu)g_3\frac{C_x C_y}{\propto^2}\left(\frac{\partial^2 h}{\partial \ni \partial \in}\right)^2\right| \\
&+\frac{(1-\mu)}{2}\left|g_3\frac{{C_x}^2}{\propto^2}\left(\frac{\partial^2 n}{\partial \ni \partial \in}\right)^2 + g_3\frac{{C_y}^2}{\propto^2}\left(\frac{\partial^2 n}{\partial \ni \partial \in}\right)^2\right| \\
&+\left|g_1\frac{C^2}{\propto^4}\left(\frac{\partial^2 n}{\partial \in^2}\right)^2 - 2g_2\frac{CC_y}{\propto^4}\left(\frac{\partial^2 h}{\partial \in^2}\right)^2 + g_3\frac{{C_y}^2}{\propto^4}\left(\frac{\partial^2 h}{\partial \in^2}\right)^2\right| \\
&+\left|\frac{(1-\mu)}{2}\beta^2 g_4 {C_x}^2\left(\frac{\partial n}{\partial \ni}\right)^2 + \frac{(1-\mu)}{2}.\frac{\beta^2 g_4 {C_y}^2}{\propto^2}\left(\frac{\partial n}{\partial \in}\right)^2\right|\Bigg] ab\partial R\partial Q \\
&-\int_0^1\int_0^1 wCn\, ab\partial \ni \partial \in
\end{aligned} \tag{29}
$$

Let:

$$s_1 = \int_0^1\int_0^1\left(\frac{d^2 n}{d \ni^2}\right)^2 d \ni d \in \tag{30}$$

$$s_2 = \int_0^1\int_0^1\left(\frac{d^2 n}{d \ni d \in}\right)^2 d \ni d \in \tag{31}$$

$$s_3 = \int_0^1\int_0^1\left(\frac{d^2 n}{d \in^2}\right)^2 d \ni d \in \tag{32}$$

$$s_4 = \int_0^1\int_0^1\left(\frac{dn}{d \ni}\right)^2 d \ni d \in \tag{33}$$

$$s_5 = \int_0^1\int_0^1\left(\frac{dn}{d \in}\right)^2 d \ni d \in \tag{34}$$

$$s_6 = \int_0^1\int_0^1 n.d \ni d \in \tag{35}$$

where the $s_1, s_2, s_3, s_4, s_5$ $and$ $s_6$ are the stiffness coefficients.

Therefore, differentiating the total potential energy (∄) with respect to the coefficient of deflection ($C$), coefficient of shear deformation with respect to x-axis ($C_x$) and coefficient of shear deformation with respect to y-axis ($C_y$):

$$\frac{\partial ∄}{\partial C} = \frac{\partial ∄}{\partial C_x} = \frac{\partial ∄}{\partial C_y} = 0 \tag{36}$$

These gives the three Equations of equilibrium as presented in Equation (29), (30) and (31):

$$
\begin{aligned}
\int_0^1\int_0^1\left[Cg_1\left(s_1+\frac{2}{\propto^2}s_2+\frac{1}{\propto^4}s_3\right) - C_x g_2\left(s_1+\frac{1}{\propto^2}s_2\right) - C_y g_2\left(\frac{1}{\propto^2}s_2+\frac{1}{\propto^4}s_3\right)\right] d \ni d \in \\
= \frac{wa^4}{D}\int_0^1\int_0^1 s_6.d \ni d \in
\end{aligned} \tag{37}
$$

$$\int_0^1\int_0^1\left[-Cg_2\left(s_1+\frac{1}{\propto^2}s_2\right)+C_x\left(g_3s_1+\frac{(1-\mu)}{2\propto^2}g_3s_2+\frac{(1-\mu)}{2}\beta^2g_4s_4\right)\right.$$
$$\left.+C_y\frac{(1+\mu)}{2\propto^2}g_3s_2\right]d\ni d\in=0 \quad (38)$$

$$\int_0^1\int_0^1\left[-Cg_2\left(\frac{1}{\propto^2}s_2+\frac{1}{\propto^4}s_3\right)+C_xg_3\frac{(1+\mu)}{2\propto^2}s_2+C_yg_3\frac{(1-\mu)}{2}\left(\frac{1}{\propto^2}s_2+\frac{1}{\propto^4}s_3\right)\right.$$
$$\left.+C_yg_4\frac{(1-\mu)}{2\propto^2}\beta^2s_5\right]d\ni d\in=0 \quad (39)$$

The three Equations of equilibrium is presented in matrix form as:

$$\begin{bmatrix}t_{11} & t_{12} & t_{13}\\ t_{21} & t_{22} & t_{23}\\ t_{31} & t_{32} & t_{33}\end{bmatrix}\begin{bmatrix}C\\ C_x\\ C_y\end{bmatrix}=\frac{wa^4}{D}\begin{bmatrix}s_6\\ 0\\ 0\end{bmatrix} \quad (40)$$

Let:

$$t_{11}=g_1\left(s_1+\frac{2}{\propto^2}s_2+\frac{1}{\propto^4}s_3\right) \quad (41)$$

$$t_{12}=-g_2\left(s_1+\frac{1}{\propto^2}s_2\right) \quad (42)$$

$$t_{13}=-g_2\left(\frac{1}{\propto^2}s_2+\frac{1}{\propto^4}s_3\right) \quad (43)$$

$$t_{21}=-g_2\left(s_1+\frac{1}{\propto^2}s_2\right) \quad (44)$$

$$t_{22}=\left(g_3s_1+\frac{(1-\mu)}{2\propto^2}g_3s_2+\frac{(1-\mu)}{2}\beta^2g_4s_4\right) \quad (45)$$

$$t_{23}=g_3\frac{(1+\mu)}{2\propto^2}s_2 \quad (46)$$

$$t_{31}=-g_2\left(\frac{1}{\propto^2}s_2+\frac{1}{\propto^4}s_3\right) \quad (47)$$

$$t_{32}=g_3\frac{(1+\mu)}{2\propto^2}s_2 \quad (48)$$

$$t_{33}=\left(g_3\frac{(1-\mu)}{2}\left(\frac{1}{\propto^2}s_2+\frac{1}{\propto^4}s_3\right)+g_4\frac{(1-\mu)}{2\propto^2}\beta^2s_5\right) \quad (49)$$

Solving the matrix in the Equation (40), gives Equation (50), (51) and (52):

$$C=\frac{wa^4}{D}(k) \quad (50)$$
$$C_x=CM_2 \quad (51)$$
$$C_y=CM_3 \quad (52)$$

where:

$$M_2=\frac{t_{21}.t_{33}-t_{23}.t_{31}}{t_{22}.t_{33}-t_{23}.t_{32}} \quad (53)$$

$$M_3=\frac{t_{21}.t_{32}-t_{22}.t_{31}}{t_{23}.t_{32}-t_{22}.t_{33}} \quad (54)$$

$$k=\frac{s_6}{t_{11}M_1-t_{12}M_2-t_{13}M_3} \quad (55)$$

## 2.5. Displacement, Stresses and Stress Resultant Analysis of the Plate

The expressions for the moment $(M_x \, and \, M_y)$, shear force $(Q_x \, and \, Q_y)$, in-plane displacement $(u \, and \, v)$, deflection (Ս) and stress of isotropic rectangular thick plate were derived according to Onyeka and Edozie (2020) by substituting the values of Ꞇ, $Ꞇ_x \, and \, Ꞇ_y$ as obtained from the previous section.

Substituting Equation (50) into (26), gave:

$$Ս = \bar{Ꞇ} n \left(\frac{wa^4}{D}\right) \tag{56}$$

where:

$$\bar{Ꞇ} = k$$

$$D = \frac{Et^3}{12(1-\mu^2)} \tag{57}$$

The bending moment along x-axes:

$$M_x = \left(-g_1 \bar{Ꞇ}\left[\frac{d^2n}{d\ \ni^2} + \mu \frac{d^2n}{d\ \in^2}\right] + g_2\left[\overline{Ꞇ_x}\frac{d^2n}{d\ \ni^2} + \mu \overline{Ꞇ_y}\frac{d^2n}{d\ \in^2}\right]\right) wa^2 \tag{58}$$

That is:

$$M_x = \overline{M_x} wa^2 \tag{59}$$

where:

$$\overline{M_x} = -g_1 \bar{Ꞇ}\left[\frac{d^2n}{d\ \ni^2} + \mu \frac{d^2n}{d\ \in^2}\right] + g_2\left[\overline{Ꞇ_x}\frac{d^2n}{d\ \ni^2} + \mu \overline{Ꞇ_y}\frac{d^2n}{d\ \in^2}\right] \tag{60}$$

where:

$$\overline{Ꞇ_x} = M_2 \bar{Ꞇ} \tag{61}$$

$$\overline{Ꞇ_y} = M_3 \bar{Ꞇ} \tag{62}$$

The bending moment along y-axes:

$$M_y = \left(-g_1 Ꞇ\left[\frac{d^2n}{d\ \in^2} + \mu \frac{d^2n}{d\ \ni^2}\right] + g_2\left[\overline{Ꞇ_y}\frac{d^2n}{d\ \in^2} + \mu \overline{Ꞇ_x}\frac{d^2n}{d\ \ni^2}\right]\right) wa^2 \tag{63}$$

That is:

$$M_y = \overline{M_y} wa^2 \tag{64}$$

where:

$$\overline{M_y} = -g_1 Ꞇ\left[\frac{d^2n}{d\ \in^2} + \mu \frac{d^2n}{d\ \ni^2}\right] + g_2\left[\overline{Ꞇ_y}\frac{d^2n}{d\ \in^2} + \mu \overline{Ꞇ_x}\frac{d^2n}{d\ \ni^2}\right] \tag{65}$$

The shear force along x-axes:

$$Q_x = wa\left(-\bar{Ꞇ}\left[\frac{\partial^3 n}{\partial\ \ni^3} + \mu \frac{\partial^3 n}{\partial\ \in^3}\right] + \left[\overline{Ꞇ_x}\frac{\partial^3 n}{\partial\ \ni^3} + \mu \overline{Ꞇ_y}\frac{\partial^3 n}{\partial\ \in^3}\right]\right) \tag{66}$$

That is:

$$Q_x = \overline{Q_x} wa \tag{67}$$

where:

$$\overline{Q_x} - \bar{Ꞇ}\left[\frac{\partial^3 n}{\partial\ \ni^3} + \mu \frac{\partial^3 n}{\partial\ \in^3}\right] + \left[\overline{Ꞇ_x}\frac{\partial^3 n}{\partial\ \ni^3} + \mu \overline{Ꞇ_y}\frac{\partial^3 n}{\partial\ \in^3}\right] \tag{68}$$

The shear force along y-axes:

$$Q_y = wa\left(-\bar{Ꞇ}\left[\frac{\partial^3 n}{\partial\ \ni^3} + \mu \frac{\partial^3 n}{\partial\ \in^3}\right] + \left[\overline{Ꞇ_x}\frac{\partial^3 n}{\partial\ \ni^3} + \mu \overline{Ꞇ_y}\frac{\partial^3 n}{\partial\ \in^3}\right]\right) \tag{69}$$

That is:

$$Q_y = \overline{Q_y} wa \tag{70}$$

where:

$$\overline{Q_y} = -\bar{C}\left[\frac{\partial^3 n}{\partial \ni^3} + \mu\frac{\partial^3 n}{\partial \in^3}\right] + \left[\overline{C_x}\frac{\partial^3 n}{\partial \ni^3} + \mu\overline{C_y}\frac{\partial^3 n}{\partial \in^3}\right] \tag{71}$$

The in-plane displacement along x-axes:

$$u = [-\bar{C}s + \overline{C_x}S(s)]\frac{dn}{d \ni}\left(\frac{wa^4}{\beta D}\right) \tag{72}$$

The in-plane displacement along y-axes:

$$v = \frac{1}{\propto}[-\bar{C}s + \overline{C_y}S(s)]\frac{dn}{d \in}\left(\frac{twa^3}{D}\right) \tag{73}$$

The normal stress along x-axes:

$$\sigma_x = 12\left[[-\bar{C}s + \overline{C_x}S(s)]\frac{d^2 n}{d \ni^2} + \frac{\mu}{\propto^2}[-\bar{C}s + \overline{C_y}S(s)]\frac{d^2 n}{d \in^2}\right](w\beta^2) \tag{74}$$

The normal stress along y-axes:

$$\sigma_y = w\beta^2\left[12\left[\mu[-\overline{Cs} + C_x S(s)]\frac{d^2 n}{d \ni^2}\right] + \frac{\mu}{\propto^2}[-\bar{C}s + \overline{C_y}S(s)]\frac{d^2 n}{d \in^2}\right] \tag{75}$$

The shear stress along x-y axes:

$$\tau_{xy} = 6\frac{(1-\mu)}{\propto}\left[-2\bar{C}s + \overline{C_x}S(s) + \overline{C_y}S(s).\frac{1}{\propto}\right]\frac{d^2 n}{\partial \ni \partial \in}(w\beta^2) \tag{76}$$

The shear stress along x-z axes:

$$\tau_{xz} = 6(1-\mu)\overline{C_x}\frac{dS(z)}{dz}\frac{dn}{d \ni}(w\beta^2) \tag{77}$$

The shear stress along y-z axes:

$$\tau_{yz} = \frac{6(1-\mu)}{\propto}\overline{C_y}\frac{dS(z)}{dz}\frac{dn}{d \in}(w\beta^2) \tag{78}$$

## 2.6 Numerical Problem

The particular shape function for rectangular plate with their respective boundary is shown in Figure 2.

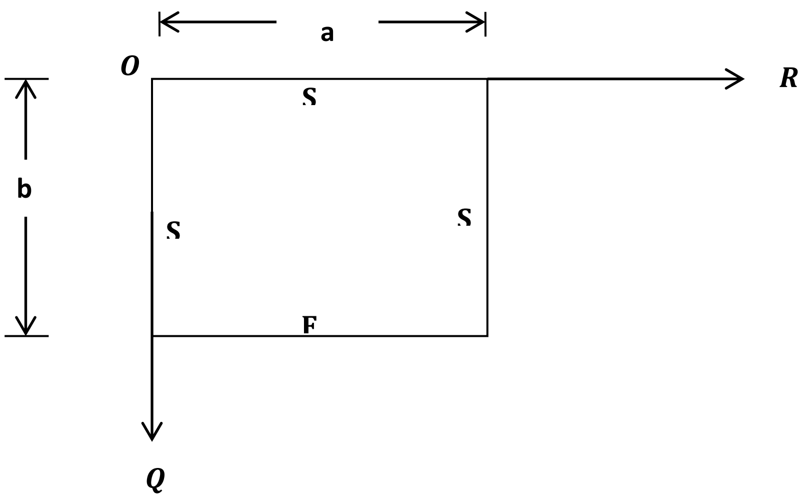


**Figure 2:** SSFS rectangular plate

Considering Figure 2, the numerical analysis of SSFS rectangular plate at various span-thickness SSFS rectangular plate was derived according to Onyeka *et al.* (2019) as presented in Equation 79:

$$\cup_{(\ni,\in)} = \left(a_0 + a_1 \ni + \frac{a_2 \ni^2}{2} + \frac{a_3 \ni^3}{6} + \frac{\ni^4}{24} F_{a4}\right) \cdot \left(\frac{b_2 \in^2}{2} + \frac{b_3 \in^3}{6} + \frac{\in^4}{24} F_{b4} + \frac{b_5 \in^5}{120}\right) \quad (79)$$

At $\ni = \in = 0; \cup = 0$ (80)

At $\ni = \in = 1; M_x \text{ and } M_y \left(ie. \frac{d^2\cup}{d\ni^2} = \frac{d^2\cup}{d\in^2} = 0\right)$ (81)

At $\ni = \in = 1; \cup = 0$ (82)

At $\in = 0; Slope \left(ie. \frac{d\cup}{d\in} = \frac{2}{3b_5}\right)$ (83)

At $\in = 0; Q_x \text{ and } Q_y \left(ie. \frac{d^3w}{dQ^3} = 0\right)$ (84)

Substituting Equations (80 to 84) into Equation (79) and solving gives the following constants:

$$a_0 = 0;\ a_1 = \frac{F_{a4}}{24};\ a_2 = 0;\ a_3 = \frac{-F_{a4}}{2} \text{ and } b_0 = 0;\ b_1 = -\frac{7}{3} b_5;\ b_2 = 0;\ b_3 = \frac{b_5}{6};\ F_{b4} = -\frac{2b_5}{3} \quad (85)$$

Substituting the constants of Equation (85) into Equation (79) gives;

$$\cup = \frac{F_{a4}}{24}(R - 2R^3 + R^4) \times \frac{b_5}{360}(7Q - 10Q^3 + 10Q^4 - 3Q^5) \quad (86)$$

That is:

$$\cup = \frac{F_{a4} \times b_5}{8640}(\ni - 2\ni^3 + \ni^4) \times \left(\frac{7\in}{3} - \frac{10}{3}\in^3 + \frac{10}{3}\in^4 - \in^5\right) \quad (87)$$

Recall from Equation 26, that;

$\cup = n.C$

Therefore:

$$C = \frac{1}{8640}(F_{a4} \times b_5) \quad (88)$$

and;

$$n = (\ni - 2\ni^3 + \ni^4) \times \left(\frac{7\in}{3} - \frac{10}{3}\in^3 + \frac{10}{3}\in^4 - \in^5\right) \quad (89)$$

Therefore:

$$\cup = \frac{F_{a4} \cdot b_5}{8640}(\ni - 2\ni^3 + \ni^4) \times \left(\frac{7\in}{3} - \frac{10}{3}\in^3 + \frac{10}{3}\in^4 - \in^5\right) \quad (90)$$

## 2. Results and Discussion

The numerical results of stiffness coefficient of the plate as obtained from Equation (30) to (35) are presented in the Table 1.

**Table 1:** Values of stiffness coefficient, s for various support (boundary conditions)

| Theory | Plate | $s_1$ | $s_2$ | $s_3$ | $s_4$ | $s_5$ | $s_6$ |
|---|---|---|---|---|---|---|---|
| Present (NRPT) | SSFS | 4.0257816 | 1.0331065 | 0.1874528 | 0.4073707 | 0.1046611 | 0.16700 |

Table 2 contains the result of bending moment, shear force and their resultants of a square SSFS rectangular plate at different span to thickness aspect ratio. These numerical values were obtained from the Equation (56) to (71).

Studying the results as presented in the Tables 2, it is shown that the non-dimensional out-of-plane displacement (Ū), bending moment ($M_x$ and $M_y$) and shear force ($Q_x$ and $Q_y$) decreases as the span to thickness ratio increases. This decrease continue until failure occurs in the plate structure. This means that, the load that causes the plate to deflect also causes the plate material to bend simultaneously. It is observed that the value of deflection varies less as the span to thickness increase, this becomes constant and equal to the value of CPT at span to thickness ratio of 90.

Tables 2 to 5 show that the value of deflection (Ū) decrease with increases in the value of the span-thickness ratio. It is also observed in the Tables that the displacement (u, v and Ū) and stresses characteristics increase as the value of the length to breadth ratio increases. This means that, the in-plane displacement are functions of x, y and z as it vary with the plate thickness while the deflection is only a function of x and y and did not varies linearly with the thickness of the plate thickness.

**Table 2:** Bending Moments, Shear Force and Stress resultants of SSFS plate for b/a = 1. 0

| | Ū (m) | $M_x$ $(kNm)$ | $M_y (kNm)$ | $Q_x$ $(kN)$ | $Q_y$ $(kN)$ |
|---|---|---|---|---|---|
| β | Ū | $\overline{M_x}$ | $\overline{M_y}$ | $\overline{Q_x}$ | $\overline{Q_y}$ |
| 4 | 0.010037 | 0.799188 | 0.430417 | 0.071685 | 0.151504 |
| 5 | 0.009371 | 0.799611 | 0.429855 | 0.063705 | 0.134751 |
| 6 | 0.009013 | 0.799846 | 0.429543 | 0.059413 | 0.125742 |
| 7 | 0.008798 | 0.799990 | 0.429352 | 0.056839 | 0.120340 |
| 8 | 0.008659 | 0.800084 | 0.429227 | 0.055174 | 0.116847 |
| 9 | 0.008564 | 0.800149 | 0.429141 | 0.054035 | 0.114458 |
| 10 | 0.008496 | 0.800195 | 0.429079 | 0.053221 | 0.112751 |
| 15 | 0.008336 | 0.800306 | 0.428932 | 0.051299 | 0.105579 |
| 20 | 0.008280 | 0.800345 | 0.428880 | 0.050628 | 0.105546 |
| 25 | 0.008254 | 0.800363 | 0.428856 | 0.050317 | 0.105530 |
| 30 | 0.008240 | 0.800373 | 0.428843 | 0.050149 | 0.105522 |
| 35 | 0.008231 | 0.800379 | 0.428835 | 0.050047 | 0.105517 |
| 40 | 0.008226 | 0.800383 | 0.428830 | 0.049981 | 0.105514 |
| 45 | 0.008222 | 0.800386 | 0.428826 | 0.049936 | 0.105511 |
| 50 | 0.008219 | 0.800387 | 0.428824 | 0.049903 | 0.105510 |
| 55 | 0.008217 | 0.800389 | 0.428822 | 0.049879 | 0.105509 |
| 60 | 0.008216 | 0.800390 | 0.428820 | 0.049861 | 0.105508 |
| 65 | 0.008215 | 0.800391 | 0.428819 | 0.049847 | 0.105507 |
| 70 | 0.008214 | 0.800391 | 0.428818 | 0.049836 | 0.105506 |
| 75 | 0.008212 | 0.800392 | 0.428817 | 0.049819 | 0.105506 |
| 80 | 0.008212 | 0.800392 | 0.428817 | 0.049819 | 0.105506 |
| 85 | 0.008212 | 0.800393 | 0.428817 | 0.049813 | 0.105505 |
| 90 | 0.008211 | 0.800393 | 0.428816 | 0.049808 | 0.105505 |
| 95 | 0.008211 | 0.800393 | 0.428816 | 0.049804 | 0.105505 |
| 100 | 0.008211 | 0.800393 | 0.428816 | 0.049800 | 0.105505 |
| CPT | 0.008211 | 0.800393 | 0.428816 | 0.049800 | 0.105505 |

From Table 3, it is shown that the non-dimensional displacement (u, v and U) characteristics decrease with increases in the value of the span-thickness ratio. It is also observed in the Tables that the displacement (u, v and U) and stresses characteristics increase as the value of the length to breadth ratio increases. This means that, the in-plane displacement are functions of x, y and z as it vary with the plate thickness while the deflection is only a function of x and y and did not varies linearly with the thickness of the plate thickness.

Similarly, it was deduced that the normal stress $(\sigma_x \, and \, \sigma_y)$ and shear stress characteristics $(\tau_{xy}, \tau_{xz} \, and \, \tau_{yz})$ also decrease as the span-thickness ratio increases. It is also observed in the Table 3 that the stresses characteristics $\left(\sigma_x, \sigma_y, \tau_{xy}, \tau_{xz} \, and \, \tau_{yz}\right)$increase as the value of the length to breadth ratio increases.

It is observed that, at span to thickness ratio between 4 and 30, the value of vertical shear stress along y and z axes $(\tau_{yz})$ varies between 0.007323 and 0.000128. These values of vertical shear stress $(\tau_{yz})$ turns to 0.0000934 and 0.0000115 at the span to thickness between 35 and 100 respectively. This value is as negligible as its equal to when corrected to 5 decimal places. The value becomes almost constant or equal to the value from CPT at span to thickness ratio of 100.

Tables 3 show that the non-dimensional displacement (u, v and U) characteristics decrease with increases in the value of the span-thickness ratio. It is also observed in the Tables that the displacement (u, v and U) and stresses characteristics increase as the value of the length to breadth ratio increases. This means that the in-plane displacement are functions of x, y and z as it vary with the plate thickness while the deflection is only a function of x and y and did not varies linearly with the thickness of the plate thickness.

Similarly, it was deduced that the normal stress $(\sigma_x \, and \, \sigma_y)$ and shear stress characteristics $(\tau_{xy}, \tau_{xz} \, and \, \tau_{yz})$ also decrease as the span-thickness ratio increases. It is also observed in the Table 3 that the stresses characteristics $\left(\sigma_x, \sigma_y, \tau_{xy}, \tau_{xz} \, and \, \tau_{yz}\right)$increase as the value of the length to breadth ratio increases.

In summary, there are two categories of rectangular plates. The plates whose vertical shear stress do not vary well from zero will be classified as thin plates because its value are almost equal to the value of the CPT. Whereas, the plate whose transverse shear stress varies very much from zero is categorized as thick plates. Therefore, the span-to-depth ratio for these categories of rectangular plates are: Thick plate:$a/t \leq 30$, while thin plate: $35 \leq a/t \geq 100$. This confirmation can be used to show the boundary between thin and thick plate (. Thus, it can be deduced from this research work that thick plate is the one whose span-depth ratio value is 4 up to 30.

**Table 3:** Displacement and Stresses of SSFS plate for length to breadth ratio of 1.0

| | $\propto = 1.0$ | | | | | | | |
|---|---|---|---|---|---|---|---|---|
| | U $(m)$ | $u\ (m)$ | $v\ (m)$ | $\sigma_x\ (kN/m)$ | $\sigma_y(kN/m)$ | $\tau_{xy}\ (kN/m)$ | $\tau_{xz}(kN/m)$ | $\tau_{yz}\ (kN/m)$ |
| β | $\bar{U}$ | $\bar{u}$ | $\bar{v}$ | $\overline{\sigma_x}$ | $\overline{\sigma_y}$ | $\overline{\tau_{xy}}$ | $\overline{\tau_{xz}}$ | $\overline{\tau_{yz}}$ |
| 4 | 0.010037 | -0.013505 | -0.005441 | 0.527400 | 0.283306 | -0.113809 | 0.019409 | 0.007323 |
| 5 | 0.009371 | -0.013067 | -0.005254 | 0.510233 | 0.273845 | -0.110005 | 0.012349 | 0.004653 |
| 6 | 0.009013 | -0.012832 | -0.005152 | 0.500997 | 0.268751 | -0.107957 | 0.008549 | 0.003219 |
| 7 | 0.008798 | -0.012691 | -0.005092 | 0.495458 | 0.265694 | -0.106727 | 0.006269 | 0.002360 |
| 8 | 0.008659 | -0.012600 | -0.005052 | 0.491875 | 0.263716 | -0.105932 | 0.004794 | 0.001804 |
| 9 | 0.008564 | -0.012537 | -0.005026 | 0.489424 | 0.262363 | -0.105388 | 0.003784 | 0.001424 |
| 10 | 0.008496 | -0.012493 | -0.005006 | 0.487674 | 0.261396 | -0.104999 | 0.003064 | 0.001152 |
| 15 | 0.008336 | -0.012387 | -0.004961 | 0.483537 | 0.259111 | -0.104080 | 0.001360 | 0.000511 |
| 20 | 0.008280 | -0.012350 | -0.004945 | 0.482093 | 0.258313 | -0.103759 | 0.000764 | 0.000287 |
| 25 | 0.008254 | -0.012333 | -0.004938 | 0.481424 | 0.257944 | -0.103610 | 0.000489 | 0.000184 |
| 30 | 0.008240 | -0.012324 | -0.004934 | 0.481062 | 0.257743 | -0.103530 | 0.000340 | 0.000128 |
| 35 | 0.008231 | -0.012319 | -0.004931 | 0.480843 | 0.257622 | -0.103481 | 0.000250 | 9.34E-05 |
| 40 | 0.008226 | -0.012315 | -0.004930 | 0.480701 | 0.257544 | -0.103449 | 0.000191 | 7.18E-05 |
| 45 | 0.008222 | -0.012312 | -0.004929 | 0.480604 | 0.257490 | -0.103428 | 0.000151 | 5.67E-05 |
| 50 | 0.008219 | -0.012311 | -0.004928 | 0.480534 | 0.257452 | -0.103412 | 0.000122 | 4.60E-05 |
| 55 | 0.008217 | -0.012309 | -0.004927 | 0.480482 | 0.257423 | -0.103401 | 0.000101 | 3.80E-05 |
| 60 | 0.008216 | -0.012308 | -0.004927 | 0.480443 | 0.257402 | -0.103392 | 8.49E-05 | 3.19E-05 |
| 65 | 0.008215 | -0.012308 | -0.004927 | 0.480413 | 0.257385 | -0.103385 | 7.23E-05 | 2.72E-05 |
| 70 | 0.008213 | -0.012307 | -0.004926 | 0.480389 | 0.257371 | -0.103380 | 6.24E-05 | 2.34E-05 |
| 75 | 0.008212 | -0.012306 | -0.004926 | 0.480353 | 0.257352 | -0.103372 | 4.78E-05 | 1.80E-05 |
| 80 | 0.008212 | -0.012306 | -0.004926 | 0.480353 | 0.257352 | -0.103372 | 4.78E-05 | 1.80E-05 |
| 85 | 0.008212 | -0.012306 | -0.004926 | 0.48034 | 0.257344 | -0.103369 | 4.23E-05 | 1.59E-05 |
| 90 | 0.008211 | -0.012305 | -0.004926 | 0.480329 | 0.257338 | -0.103367 | 3.77E-05 | 1.42E-05 |
| 95 | 0.008211 | -0.012305 | -0.004926 | 0.480319 | 0.257333 | -0.103365 | 3.37E-05 | 1.27E-05 |
| 100 | 0.008211 | -0.012305 | -0.004926 | 0.480311 | 0.257329 | -0.103363 | 3.06E-05 | 1.15E-05 |
| CPT | 0.008211 | -0.012305 | -0.004926 | 0.480311 | 0.257329 | -0.103363 | 3.06E-05 | 1.15E-05 |

Table 4 reveals that at span to thickness ratio between 4 and 25, the value of vertical shear stress along y and z axes $\tau_{yz}$ varies 0.005611 and 0.000141. These values of vertical shear stress become 0.0000981 and 0.0000109 in the span to a thickness between 30 and 85 respectively. Meanwhile, the value of vertical shear stress $\tau_{yz}$ is about 0.00000978 and 0.00000883, in the span to a thickness between 85 and 100, which is about 0.0000001 when corrected to 5 decimal places. This negligible value become almost constant or equal to the value from CPT.

In summary, there are three categories of rectangular plates. The plates whose vertical shear stress do not vary well from zero will be classified as thin plates because its value are almost equal to the value of the CPT. In between the thin and thick plate is the classified as moderate thick plate. Since the plate whose transverse shear stress varies very much from zero is categorized as thick plates. Therefore, the span-to-depth ratio for these categories of rectangular plates are: Thick plate:$a/t \leq 25$; moderately thick plate: $30 \leq a/t \leq 85$; thin plate: $a/t \geq 85$. This confirmation can be used to show the boundary between thin and thick plate (Ezeh *et al.,* 2019). Thus, it can be deduced from this research work that thick plate is the one whose span-depth ratio value is 4 up to 25.

**Table 4:** Displacement and Stresses of SSFS plate for length to breadth ratio of 1.5

| | $\propto = 1.5$ | | | | | | | |
|---|---|---|---|---|---|---|---|---|
| | U $(m)$ | $u\ (m)$ | $v\ (m)$ | $\sigma_x\ (kN/m)$ | $\sigma_y (kN/m)$ | $\tau_{xy}\ (kN/m)$ | $\tau_{xz} (kN/m)$ | $\tau_{yz}\ (kN/m)$ |
| β | $\bar{U}$ | $\bar{u}$ | $\bar{v}$ | $\overline{\sigma_x}$ | $\overline{\sigma_y}$ | $\overline{\tau_{xy}}$ | $\overline{\tau_{xz}}$ | $\overline{\tau_{yz}}$ |
| 4 | 0.012406 | -0.016876 | -0.004517 | 0.630375 | 0.258342 | -0.121237 | 0.021665 | 0.005611 |
| 5 | 0.011658 | -0.016380 | -0.004380 | 0.611797 | 0.250664 | -0.117610 | 0.013791 | 0.003570 |
| 6 | 0.011255 | -0.016112 | -0.004306 | 0.601791 | 0.246528 | -0.115655 | 0.009549 | 0.002471 |
| 7 | 0.011013 | -0.015952 | -0.004261 | 0.595787 | 0.244045 | -0.114482 | 0.007003 | 0.001812 |
| 8 | 0.010856 | -0.015848 | -0.004232 | 0.591901 | 0.242439 | -0.113723 | 0.005356 | 0.001385 |
| 9 | 0.010749 | -0.015777 | -0.004213 | 0.589242 | 0.241339 | -0.113203 | 0.004229 | 0.001094 |
| 10 | 0.010672 | -0.015726 | -0.004199 | 0.587343 | 0.240554 | -0.112832 | 0.003423 | 0.000885 |
| 15 | 0.010492 | -0.015606 | -0.004165 | 0.582853 | 0.238697 | -0.111954 | 0.001519 | 0.000393 |
| 20 | 0.010428 | -0.015564 | -0.004154 | 0.581284 | 0.238048 | -0.111647 | 0.000854 | 0.000221 |
| 25 | 0.010399 | -0.015544 | -0.004148 | 0.580559 | 0.237748 | -0.111505 | 0.000547 | 0.000141 |
| 30 | 0.010383 | -0.015534 | -0.004146 | 0.580165 | 0.237585 | -0.111428 | 0.000380 | 9.81E-05 |
| 40 | 0.010368 | -0.015523 | -0.004143 | 0.579773 | 0.237423 | -0.111352 | 0.000213 | 5.52E-05 |
| 45 | 0.010363 | -0.015521 | -0.004142 | 0.579668 | 0.237379 | -0.111331 | 0.000169 | 4.36E-05 |
| 50 | 0.010360 | -0.015519 | -0.004141 | 0.579592 | 0.237348 | -0.111316 | 0.000137 | 3.53E-05 |
| 55 | 0.010358 | -0.015517 | -0.004141 | 0.579536 | 0.237325 | -0.111305 | 0.000113 | 2.92E-05 |
| 60 | 0.010356 | -0.015516 | -0.004141 | 0.579494 | 0.237307 | -0.111297 | 9.49E-05 | 2.45E-05 |
| 65 | 0.010355 | -0.015515 | -0.004140 | 0.579461 | 0.237294 | -0.111291 | 8.08E-05 | 2.09E-05 |
| 70 | 0.010354 | -0.015514 | -0.004140 | 0.579434 | 0.237283 | -0.111285 | 6.97E-05 | 1.80E-05 |
| 75 | 0.010352 | -0.015513 | -0.004140 | 0.579396 | 0.237267 | -0.111278 | 5.34E-05 | 1.38E-05 |
| 80 | 0.010352 | -0.015513 | -0.004140 | 0.579396 | 0.237267 | -0.111278 | 5.34E-05 | 1.38E-05 |
| 85 | 0.010352 | -0.015513 | -0.004140 | 0.579381 | 0.237261 | -0.111275 | 4.73E-05 | 1.22E-05 |
| 90 | 0.0103512 | -0.015513 | -0.004140 | 0.579369 | 0.237256 | -0.111273 | 4.22E-05 | 1.09E-05 |
| 95 | 0.0103508 | -0.015512 | -0.004140 | 0.579359 | 0.237252 | -0.111271 | 3.78E-05 | 9.78E-06 |
| 100 | 0.0103505 | -0.015512 | -0.004139 | 0.579350 | 0.237248 | -0.111269 | 3.42E-05 | 8.83E-06 |
| CPT | 0.0103505 | -0.015512 | -0.004139 | 0.579350 | 0.237248 | -0.111269 | 3.42E-05 | 8.83E-06 |

Studying the results as presented in the Tables 5, it is shown that the non-dimensional displacement (u, v and U) characteristics decrease with increases in the value of the span-thickness ratio. It is also observed in the Tables that the displacement (u, v and U) and stresses characteristics increase as the value of the length to breadth ratio increases. This means that, the in-plane displacement are functions of x, y and z as it vary with the plate thickness while the deflection is only a function of x and y and did not varies linearly with the thickness of the plate thickness.

Similarly, it was deduced that the normal stress $(\sigma_x\ and\ \sigma_y)$ and shear stress characteristics $(\tau_{xy}, \tau_{xz}\ and\ \tau_{yz})$ also decrease as the span-thickness ratio increases. It is also observed in the Table 3 that the stresses characteristics $\left(\sigma_x, \sigma_y, \tau_{xy}, \tau_{xz}\ and\ \tau_{yz}\right)$increase as the value of the length to breadth ratio increases. These decreases continue until failure occurs in the plate structure.

Furthermore, from Table 5 it can be seen that at span to a thickness ratio between 4 and 25, the value of vertical shear stress along y and z axes $(\tau_{xz})$ varies between 0.004447 and

0.000112. These values of vertical shear stress become 0.0000779 and 0.0000109 in the span to a thickness between 30 and 80 respectively. Meanwhile, the value of vertical shear stress ($\tau_{yz}$) is about 0.0000097 and 4.184E-05, in the span to a thickness between 85 and 100 which is about 0.00000701 when corrected to 5 decimal places. The value become almost constant or equal to the value from CPT.

In summary, there are three categories of rectangular plates. The plates whose vertical shear stress do not vary well from zero will be classified as thin plates because its values are almost equal to the value of the CPT. In between the thin and thick plate is the classified as moderate thick plate. Since the plate whose transverse shear stress varies very much from zero is categorized as thick plates. Therefore, the span-to-depth ratio for these categories of rectangular plates are: Thick plate:$a/t \leq 25$; moderately thick plate: $30 \leq a/t \leq 80$; thin plate: $a/t \geq 80$. This confirmation can be used to show the boundary between thin and thick plate (Ezeh *et al.,* 2019). Thus, it can be deduced from this research work that thick plate is the one whose span-depth ratio value is 4 up to 25.

**Table 5:** Displacement and Stresses of SSFS plate for length to breadth ratio of 2.0

| | $\propto = 2.0$ | | | | | | | |
|---|---|---|---|---|---|---|---|---|
| | U $(m)$ | $u\ (m)$ | $v\ (m)$ | $\sigma_x\ (kN/m)$ | $\sigma_y (kN/m)$ | $\tau_{xy}\ (kN/m)$ | $\tau_{xz} (kN/m)$ | $\tau_{yz}\ (kN/m)$ |
| β | $\bar{U}$ | $\bar{u}$ | $\bar{v}$ | $\overline{\sigma_x}$ | $\overline{\sigma_y}$ | $\overline{\tau_{xy}}$ | $\overline{\tau_{xz}}$ | $\overline{\tau_{yz}}$ |
| 4 | 0.013471 | -0.018397 | -0.003688 | 0.676285 | 0.245283 | -0.09906 | 0.022623 | 0.004447 |
| 5 | 0.012689 | -0.017877 | -0.003582 | 0.657137 | 0.238316 | -0.096229 | 0.014404 | 0.002831 |
| 6 | 0.012267 | -0.017596 | -0.003525 | 0.646820 | 0.234560 | -0.094703 | 0.009975 | 0.001960 |
| 7 | 0.012014 | -0.017428 | -0.003490 | 0.640627 | 0.232306 | -0.093786 | 0.007316 | 0.001437 |
| 8 | 0.011850 | -0.017319 | -0.003468 | 0.636618 | 0.230847 | -0.093193 | 0.005595 | 0.001099 |
| 9 | 0.011738 | -0.017244 | -0.003453 | 0.633876 | 0.229849 | -0.092788 | 0.004417 | 0.000868 |
| 10 | 0.011658 | -0.017191 | -0.003442 | 0.631916 | 0.229136 | -0.092498 | 0.003576 | 0.000702 |
| 15 | 0.011469 | -0.017065 | -0.003416 | 0.627284 | 0.227450 | -0.091812 | 0.001587 | 0.000312 |
| 20 | 0.011403 | -0.017021 | -0.003407 | 0.625665 | 0.226860 | -0.091573 | 0.000893 | 0.000175 |
| 25 | 0.011372 | -0.017001 | -0.003403 | 0.624917 | 0.226588 | -0.091462 | 0.000571 | 0.000112 |
| 30 | 0.011355 | -0.016990 | -0.003400 | 0.624510 | 0.226440 | -0.091402 | 0.000397 | 7.79E-05 |
| 35 | 0.011345 | -0.016983 | -0.003399 | 0.624265 | 0.226351 | -0.091365 | 0.000291 | 5.72E-05 |
| 40 | 0.011339 | -0.016979 | -0.003398 | 0.624106 | 0.226293 | -0.091342 | 0.000223 | 4.38E-05 |
| 45 | 0.011334 | -0.016976 | -0.003398 | 0.623997 | 0.226253 | -0.091326 | 0.000176 | 3.46E-05 |
| 50 | 0.011331 | -0.016973 | -0.003397 | 0.623919 | 0.226225 | -0.091314 | 0.000143 | 2.80E-05 |
| 55 | 0.011329 | -0.016972 | -0.003397 | 0.623861 | 0.226204 | -0.091306 | 0.000118 | 2.32E-05 |
| 60 | 0.011327 | -0.016971 | -0.003397 | 0.623817 | 0.226188 | -0.091299 | 9.91E-05 | 1.95E-05 |
| 65 | 0.011326 | -0.016970 | -0.003396 | 0.623783 | 0.226175 | -0.091294 | 8.45E-05 | 1.66E-05 |
| 75 | 0.011323 | -0.016968 | -0.003396 | 0.623716 | 0.226151 | -0.091284 | 5.58E-05 | 1.09E-05 |
| 80 | 0.011323 | -0.016968 | -0.003396 | 0.623716 | 0.226151 | -0.091284 | 5.58E-05 | 1.09E-05 |
| 85 | 0.011322 | -0.016968 | -0.003396 | 0.623701 | 0.226146 | -0.091282 | 4.94E-05 | 9.70E-06 |
| 90 | 0.011322 | -0.016967 | -0.003396 | 0.623689 | 0.226141 | -0.091280 | 4.41E-05 | 8.65E-06 |
| 95 | 0.011321 | -0.016967 | -0.003396 | 0.623678 | 0.226137 | -0.091279 | 3.95E-05 | 7.76E-06 |
| 100 | 0.011321 | -0.016967 | -0.003396 | 0.623669 | 0.226134 | -0.091277 | 3.57E-05 | 7.01E-06 |
| CPT | 0.011317 | -0.016964 | -0.003395 | 0.623587 | 0.226104 | -0.091265 | 3.57E-05 | 7.01E-06 |

The result of the comparison made as presented in Table 6, Figures 3 and 4, shows that the present study predicts slightly higher values for all aspect ratios. This proves some level safety and reliability of this method as it will not put the structure into danger. The total average percentage difference between the present study and that of Ezeh *et al.* (2018) is 3862.8%. This reveals that the work of Ezeh et al. (2018) produces error and cannot be reliable for thick plate analysis. This can be proven as the total average percentage difference between the present study and that of Gwarah (2019) is 6.9%. This means that at about 93 % confidence level, the values from the present study are the same with those of Gwarah (2019). This value has been sufficient in the statistical analysis showed that the present method can be used with confidence for analysis of deflection on a SSFS rectangular plate.

**Table 6:** Comparison of results from the present work and literature values of square thick rectangular plate

| β | Present work U $(m)$ | Gwarah (2019) U $(m)$ | Percentage difference (%) | Present work U $(m)$ | Ezeh *et al.* (2019) U $(m)$ | Percentage difference (%) |
|---|---|---|---|---|---|---|
| 4 | 0.010037 | 0.009370 | 7.118463 | 0.010037 | 0.000253 | 3867.194 |
| 5 | 0.009371 | 0.008766 | 6.901666 | 0.009371 | 0.000236 | 3870.763 |
| 10 | 0.008564 | 0.007959 | 7.601457 | 0.008564 | 0.000215 | 3883.256 |
| 20 | 0.008280 | 0.007757 | 6.742297 | 0.008280 | 0.000209 | 3861.722 |
| 30 | 0.008240 | 0.007719 | 6.749579 | 0.008240 | 0.000208 | 3861.538 |
| 40 | 0.008226 | 0.007706 | 6.747989 | 0.008226 | 0.000208 | 3854.808 |
| 50 | 0.008219 | 0.007700 | 6.74026 | 0.008219 | 0.000208 | 3851.442 |
| 60 | 0.008216 | 0.007697 | 6.742887 | 0.008216 | 0.000208 | 3850.000 |
| 70 | 0.008213 | 0.007695 | 6.731644 | 0.008213 | 0.000208 | 3848.558 |
| 80 | 0.008212 | 0.007693 | 6.746393 | 0.008212 | 0.000207 | 3867.150 |
| 90 | 0.008211 | 0.007693 | 6.733394 | 0.008211 | 0.000207 | 3866.667 |
| 100 | 0.008211 | 0.007691 | 6.761149 | 0.008211 | 0.000207 | 3866.667 |
| CPT | 0.008211 | 0.007691 | 6.761149 | 0.008211 | 0.000207 | 3866.667 |
| Average % difference | | | 6.9 | | | 3862.8 |

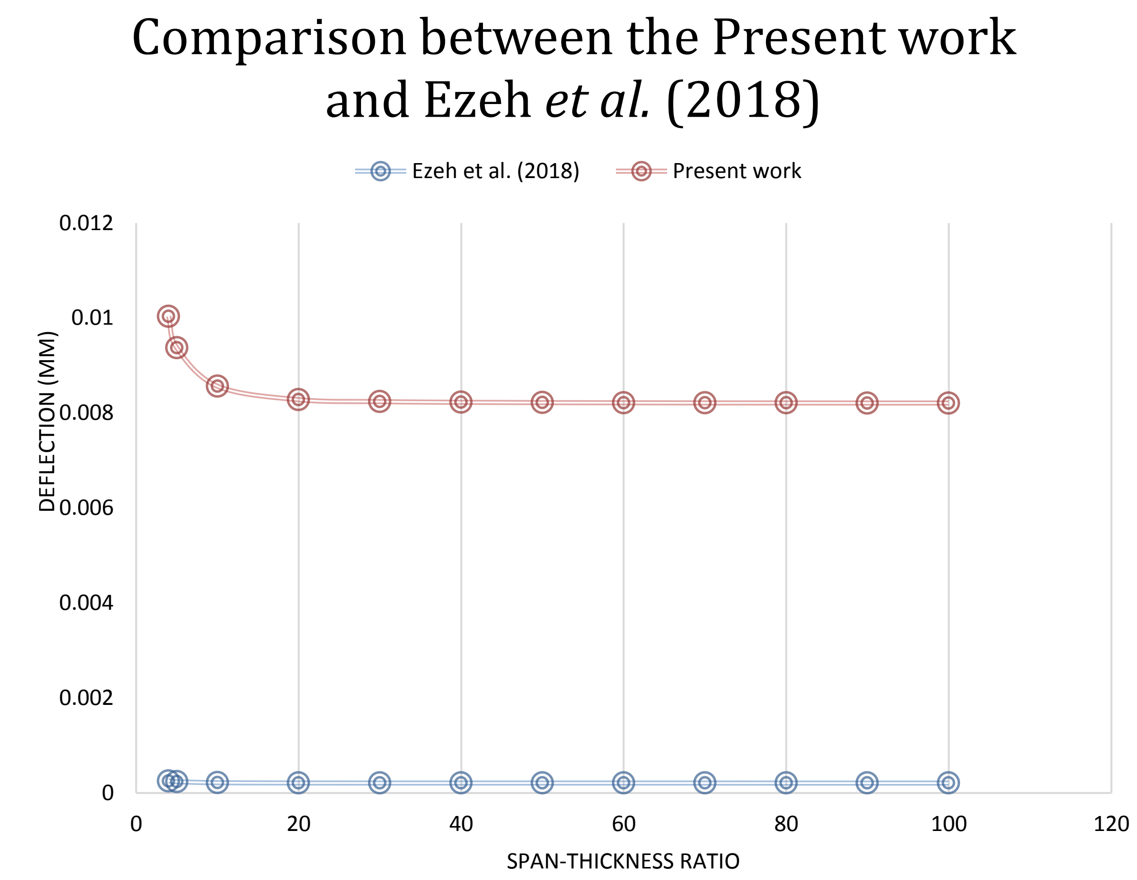


**Figure 4:** Deflection versus span to thickness ratio used to compare present work with literature

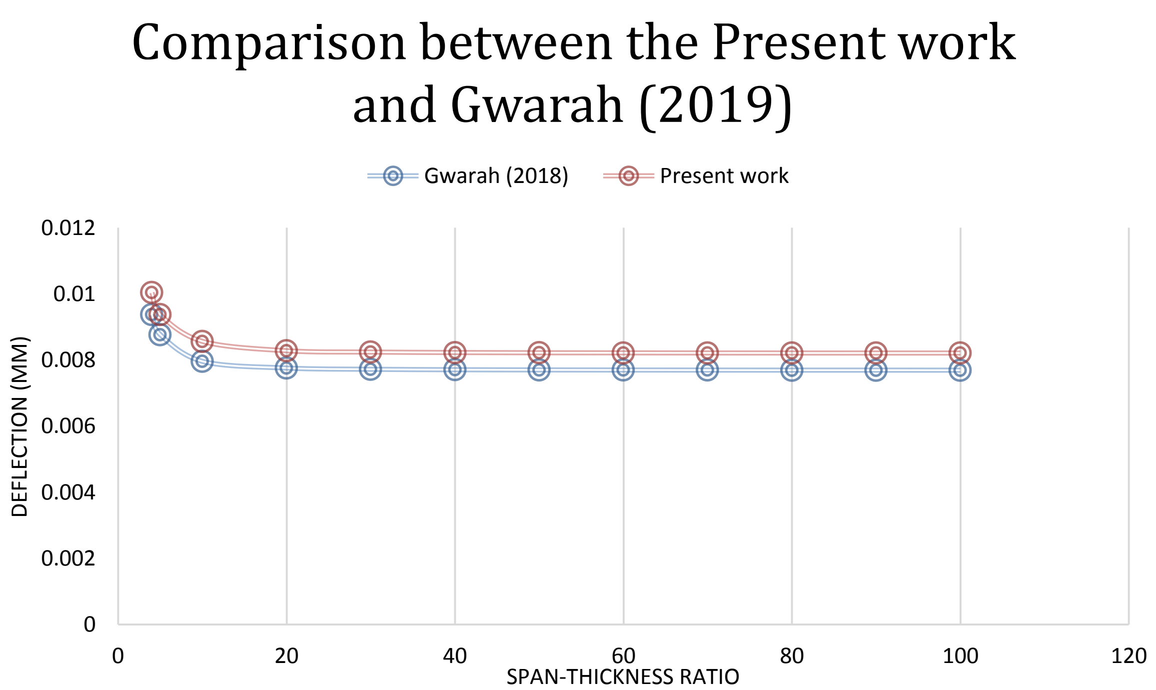


**Figure 4:** Deflection versus span to thickness ratio used to compare present work with literature

## 3. Conclusion

Application of a new refined shear deformation theory for the analysis of thick rectangular plate has been investigated with the following conclusion:

i. The values of the transverse shear stresses obtained by this theory achieve accepted transverse shear stress to the thickness of plate variation and satisfied the transverse flexibility of condition of the plate while predicting the be characteristics for the CSSS isotropic rectangular thin or thick plate.
ii. The governing differential equations and associated boundary conditions obtained are variationally consistent and can be used with confidence in the analysis of isotropic rectangular.
iii. The deflection and stresses obtained by present theory are in good agreement with the other order theories. This validates the efficacy and reliability of the present new refined plate theory (NRPT).

## References

Aghdam, MM. and Vafa, JP. 2004. Bending analysis of thick rectangular plates with various boundary conditions using extended Kantorovich method. Lecture Series on Computer Science Publishers and Computational Sciences, 1: 1- 4.

Chandrashekhara, K. 2001. Theory of Plates. University Press (India) Limited, New Delhi.

Ezeh, JC., Ibearugbulem, OM., Ettu, LO., Gwarah, LS. and Onyechere, IC. 2018. Application of shear deformation theory for analysis of CCCS and SSFS rectangular isotropic thick plates. Journal of Mechanical and Civil Engineering (IOSR-JMCE), 15(5): 33 – 42.

Ghugal, YM. and Gajbhiye, PD. 2016. Bending analysis of thick isotropic plates by using 5th order shear deformation theory. Journal of Applied and Computational Mechanics, 2(2): 80-95.

Gujar, PS. and Ladhane, KB. 2015. Bending analysis of simply supported and clamped circular plate. International Journal of Civil Engineering (SSRG-IJCE), 2(5): 45 – 51.

Gwarah, LS. 2019. Application of Shear Deformation Theory in the Analysis of Thick Rectangular Plates using Polynomial Displacement Functions. PhD thesis, Federal University of Technology, Owerri, Nigeria.

Hoang, NN., Hong, TT., Vinh, PV., Quang, ND. and Thom, DV. 2019. A refined simple first-order shear deformation theory for static bending and free vibration analysis of advanced composite plates. Materials (Basel), 12(15): 2385.

Ibearugbulem, OM., Ezeh, JC. and Ettu, LO. 2013. Pure bending analysis of thin rectangular SSSS plate using Taylor-Mclaurin series. International Journal of Civil and Structural Engineering, 3(4): 685 – 691.

Ibearugbulem, OM., Ezeh, JC., Ettu, LO. and Gwarah, LS. 2018. Bending analysis of rectangular thick plate using polynomial shear deformation theory. IOSR Journal of Engineering, 8(9): 53-61.

Ibearugbulem, OM., Njoku, KO. and Eziefula, UG. 2016. Full Shear Deformation for Analysis of Thick Plate. Proceedings of Academics World 43rd International Conference, Rome, Italy, 2nd-3rd September, 38-46.

Kirchhoff, GR. 1850. U"ber die Schwingungen einer kriesformigen elastischen scheibe. Annalen der Physik und Chemie, 81: 258 - 264 (in German).

Liessa, AW. 1973. The free vibration of rectangular plates. Journal of Sound Vibration, 31: 257–293.

Onyechere, IC. Ibearugbulem, OM. Anya, UC. Anyaogu, L. and Awodiji, CTG. 2020. Free-vibration study of thick rectangular plates using polynomial displacement functions. Saudi Journal of Engineering and Technology, 4(1): 38-46.

Onyeka, FC. and Edozie, OT. 2020. Application of higher order shear deformation theory in the analysis of thick rectangular plate. International Journal on Emerging Technologies, 11(5): 62–67.

Onyeka, FC., Okafor, FO. and Onah, HN. 2018. Displacement and stress analysis in shear deformable thick plate. International Journal of Applied Engineering Research, 13(11): 9893 – 9908.

Onyeka, FC., Okeke, TE. and Wasiu, J. 2020. Strain–displacement expressions and their effect on the deflection and strength of plate. Advances in Science, Technology and Engineering Systems, 5(5): 401-413.

Ozioko, HO., Ibearugbulem, OM., Ezeh, JC. and Anya, UC. 2019. Algorithm for Exact Solution of Thick Anisotropic Plates Scholar Journal of Applied Sciences and Research, 2(4): 11 – 25.

Reissner, E. 1945. The Effect of transverse shear deformation on the bending elastic plate. Transactions of the American Society of Mechanical Engineers, Journal of Applied Mechanics, 12: 69 - 77.

Roknuzzaman, Md., Hossain, BMd., Rashedu, H. and Tarif, UA. 2015. Analysis of rectangular plate with opening by finite difference method. American Journal of Civil Engineering and Architecture, 3(5): 165-173.

Sayyad, II., Chikalthankar, SB. and Nandedkar, VM. 2013. Bending and free vibration analysis of isotropic plate using refined plate theory. Bonfring International Journal of Industrial Engineering and Management Science, 3(2): 40 – 46.

Sayyad, AS., Shinde, BM. and Ghugal, YM. 2015. Thermo-elastic bending analysis of laminated composite plates according to various shear deformation theories. Open Engineering, formerly Central European Journal of Engineering, 5(1): 18-30.

Shwetha, K. Subrahmanya, V. and Bhat, P. 2018. Comparison between thin plate and thick plate from Navier solution using Matlab software. International Research Journal of Engineering and Technology (IRJET), 5(6): 2675 – 2680.

Timoshenko, SP. and Woinowsky-Krieger, S. 1959. Theory of plates and shells. McGraw-Hill/Springer; New York, NY, USA.

Touratier, M. 1991. An efficient standard plate theory. International Journal of Engineering Science, 29(8): 901–16.

Yang, Z. and Qian, X. 2017. Analysis bending solutions of clamped rectangular thick plate. Hindawi Mathematical Problems in Engineering, 20: 1-6